Response of rat intracranial 9L gliosarcoma to microbeam radiation therapy[1]

F. Avraham Dilmanian,[2] Terry M. Button, Géraldine Le Duc,[3] Nan Zhong, Louis A. Pe a, Jennifer A.L. Smith, Steve R. Martinez, Tigran Bacarian, Jennifer Tammam,[4] Baorui Ren,[5] Peter M. Farmer, John Kalef-Ezra, Peggy L. Micca, Marta M. Nawrocky, James A. Niederer, F. Peter Recksiek, Alexander Fuchs, and Eliot M. Rosen

Brookhaven National Laboratory, Upton, NY 11973 (F.A.D., G.L.D., N.Z., L.A.P., T.B., J.T., B.R., P.L.M., M.M.N., J.A.N., F.P.R.); State University of New York, Stony Brook, NY 11794 (T.M.B., S.R.M.); Long Island Jewish Medical Center, New Hyde Park, NY 11040 (P.M.F., A.F., E.M.R); University of Ioannina, 45110 Ioannina, Greece (J.K.-E.); and Pharmacyclics, Inc., Sunnyvale, CA 94086 (J.A.L.S.)

Radiotherapeutic doses for malignant gliomas are generally palliative because greater, supposedly curative doses would impart clinically unacceptable damage to nearby vital CNS tissues. To improve radiation treatment for human gliomas, we evaluated microbeam radiation therapy, which utilizes an array of parallel, microscopically thin (<100 μm) planar beams (microbeams) of synchrotron-generated X rays. Rats with i.c. 9L gliosarcoma tumors were exposed laterally to a single microbeam, 27 μm wide and 3.8 mm high, stepwise, to produce irradiation arrays with 50, 75, or 100 μm of on-center beam spacings and 150, 250, 300, or 500 Gy of in-slice, skin-entrance, single-exposure doses. The resulting array size was 9 mm wide and 10.4 mm high (using three 3.8-mm vertical tiers); the beam's median energy was ~70 keV. When all data were collated, the median survival was 70 days; no depletion of nerve cells was observed. However, when data from the highest skin-entrance dose and/or the smallest microbeam spacings were excluded, the median survival time of the subset of rats was 170 days, and no white matter necrosis was observed. Others have reported unilateral single-exposure broad-beam irradiation of i.c. 9L gliosarcomas at 22.5 Gy with a median survival of only ~34 days and with severe depletion of neurons. These results suggest that the therapeutic index of unidirectional microbeams is larger than that of the broad beams and that an application for microbeam radiation therapy in treating certain malignant brain tumors may be found in the future. *Neuro-Oncology 4, 26-38, 2002 (Posted to Neuro-Oncology [serial online], Doc. 01-041, December 6, 2001. URL <neuro-oncology.mc.duke.edu>)*

Received 18 July 2001, accepted 8 October 2001.

[1]This work was supported by the Children's Brain Tumor Foundation, New York, NY, and by the U.S. Department of Energy under contract DE-AC02-76CH00016 with Brookhaven National Laboratory.

[2]Address correspondence and reprint requests to F. Avraham Dilmanian, Medical Department, Bldg. 490, Brookhaven National Laboratory, Upton, NY 11973-5000.

[3]Present address: European Synchrotron Radiation Facility, BP-220, Grenoble, France.

[4]Present address: Ilex Oncology, 20 Overland St., Boston, MA 02215.

[5]Present address: Nortel Networks, Wilmington, MA 01887.

[6]Abbreviations used are as follows: 9LGS, 9L gliosarcoma; BNL, Brookhaven National Laboratory; MRT, microbeam radiation therapy; NSLS, National Synchrotron Light Source.

The incident rate of all primary malignant brain tumors is 16,500 cases a year in the United States (CBTRUS, 2000). Radiation therapy, the primary method of treating these tumors, is generally palliative rather than curative in treating high-grade gliomas (Mornex et al., 1993). Treatment failure is primarily related to constraints on the delivery of adequate radiation dose to the tumor, which is due to the limitations of normal tissue tolerance. MRT,[6] a novel technique developed at the NSLS, BNL (Slatkin et al., 1992, 1995a), appears to address this problem. Previous studies suggest that unidirectional single-fraction MRT can preferentially kill an i.c. rat glioma, namely 9LGS, while sparing

the normal brain tissue (Laissue et al., 1998; Slatkin et al., 1995b). MRT utilizes arrays of parallel, microscopically thin (<100 μm) planar slices of synchrotron-generated X rays (microplanar beams, microbeams) and is commonly administered in a single dose. Other than at the NSLS—where microbeam irradiation studies of normal rat brain (Slatkin et al., 1995a), rat 9LGS brain tumors (Laissue et al., 1998; Slatkin et al., 1995b), and normal duck embryo brains (Dilmanian et al., 2001) have been pursued—MRT-related research has also been conducted at the European Synchrotron Radiation Facility, Grenoble, France, since 1995, where tolerances to microbeam irradiation of the cerebella of suckling rats (Laissue et al., 1999) and immature pigs (Laissue et al., 2001) have been evaluated.

Synchrotron X rays are produced when relativistic electrons in storage rings pass through strong magnetic fields (Winick, 1980). Their characteristics include a broad continuous spectrum, a natural forwardly peaked collimation (producing a quasiparallel beam), very high intensity, and small effective source size. These properties allow the production of very narrow and intense beams. The beam energies used in previous NSLS studies had a maximum of 120-keV median energy, using gadolinium or copper beam filtration to preferentially attenuate mostly the lower part of the spectrum. Increased beam filtration raises the spectral energy and reduces the incident dose rate of the beam. The spectral energy also influences the "valley" dose in the microbeam array (the radiation leakage between microbeams).

The tissue-sparing effect of X-ray microbeams was first evaluated by Slatkin et al. (1995a), who irradiated rat brain with synchrotron-generated planar microbeams. These studies showed that a parallel array of 10 to 20 microplanar beams of 27-μm beam width and 75- or 100-μm beam spacing, center to center, did not cause tissue necrosis when used at in-slice entrance doses of up to 5000 Gy, although it did cause loss of neuronal and astrocytic cell nuclei in the direct paths of the microbeams. It was suggested that endothelial cells, and perhaps oligodendroglial cells, surviving between microbeams might be able to replace the cells lethally injured in the direct paths of the X-ray microplanar beams (Slatkin et al., 1995a).

The tolerance of the immature CNS to microbeams was studied both at the European Synchrotron Radiation Facility and the NSLS to evaluate the potential of MRT in pediatric neuro-oncology. At the European Synchrotron Radiation Facility, 11-day-old and 13-day-old (suckling) rats exposed once to unidirectional microbeams (28-μm width and 105- or 210-μm spacing) in their hind brains at up to a 150-Gy dose (Laissue et al., 1999) showed only some temporary delay in weight gain. At the NSLS, duck embryos were exposed 3 to 4 days prior to hatching (Dilmanian et al., 2001). Single exposures to either microbeams (27-μm beam width, 100-μm beam spacing) or broad beams were used. For 160-Gy microbeams (in-slice, in-depth dose), long-term survival with no ataxia and no histologically detectable brain damage was observed, whereas ducks irradiated with 18-Gy broad beams all died of ataxia within 90 days, with brain damage evident in some. This showed about a 10-fold higher tolerance to the microbeams than did broad beams—about 2.7-fold when the in-slice dose was normalized to the entire irradiation area.

The therapeutic effects of unidirectional and bidirectional X-ray microbeams were observed first in a study on rat brain 9LGS reported in part by Slatkin et al. (1995b) and in part by Laissue et al. (1998). The experiment used stepwise irradiations with a 27 μm–wide microbeam to produce microbeam exposure arrays (single dose) with 100- or 200-μm spacing between the irradiated microplanar beams and 50-keV median beam energy. The survivals achieved by day 220 postinoculation were 4 of 14 with 625-Gy unidirectional microbeams and 8 of 15 with 625-Gy bidirectional irradiations. Histopathologic analysis of the brains in both groups up to ~310 days postirradiation revealed little brain damage for the normal brain regions traversed by a single array, but some loss of tissue structure was noted in the cross-fired zones (Laissue et al., 1998).

In the investigation reported here, several beam spacings and doses that had not been used previously were used for unidirectional MRT of the 9LGS. We assessed the dependence of tumor control and normal tissue damage on beam spacing and dose. The results are compared to those from a broad-beam X-ray therapy experiment by other investigators at BNL (Joel et al., 1990) who used the same 9LGS cell line (called the *BNL 9LGS* cell line). The comparison allowed us to evaluate the therapeutic index (the ratio of the maximum dose tolerated by normal tissue to the dose required for tumor control) for unidirectional MRT of this particular tumor.

Materials and Methods

Tumor Inoculations

The BNL strain of the intracerebral rat 9LGS (Joel et al., 1990) was established from cultured gliosarcoma cells originally derived by Schmidek et al. (1971). These tumor cells were maintained in Dulbecco's modified Eagle's medium supplemented with 5% fetal bovine serum. All procedures involving animals were approved by the Institutional Animal Care and Use Committee at BNL. Briefly, 8-week-old male Fischer 344 rats (Taconic Farms, Germantown, N.Y.) were injected with 1×10^4 cultured cells in 1 μl of medium into the left frontal lobe of the brain. For this, the scalp of the anesthetized rat was aseptically incised, and a 0.5-mm burr hole was made at a position 4 mm to the left of the midline and directly on the bregma. The cells were implanted 5 mm beneath the surface of the skull using a 27-gauge needle fitted with a depth-limiting plastic collar. Under these conditions, the diameter of the tumor at day 14 was 35 to 40 mg (Joel et al., 1990), which, assuming a tumor density of 1.0 g/cc, relates to 4.1-4.2 mm in diameter. No pretreatment tumor size measurement was carried out. The median survival time of unirradiated tumor-bearing rats, using this model at BNL, was 20 ± 3 days (mean ± SD; Coderre et al., 1994a).

Microbeam Irradiations

The technical aspects of microbeam irradiations at the X17B1 beamline of the NSLS have been described elsewhere (Slatkin et al., 1995a). The ring was operated at 2.584 GeV and the wiggler at 4.7 teslas. The beam was filtered with 3-mm water-cooled silicon and 0.25- or 0.51-mm copper. A vertical microbeam 27 μm in width and 3.8 mm in height was produced from a broad beam using a single-slit collimator made of 6 mm–thick tantalum. The animals were positioned prone, with the back of their heads horizontal. They were irradiated laterally, from right side to left, in a stepwise procedure. After exposure to a single microbeam as described above, the animals were stepped laterally to the beam by the prescribed beam spacing values (50, 75, or 100 μm) using a computer-controlled translational stage with a 1-μm step size. A single 3.8-mm high microbeam array, 8 to 10 mm wide, was administered in this way. The microbeam array height of 11.4 mm (about 10.4 mm of which traversed the brain) was achieved by irradiating the brain with 3 such tiers, one over the other. The average incident dose rates were ~500 and ~830 Gy/s for the 0.51-mm and the 0.25-mm copper filters, respectively.

Targeting of the brain tumor with the microbeam array was aided by X-ray fluorescent radiography. For targeting of the tumor laterally, the radiographs were used to relate the position of the beam to the lateral location of anatomical landmarks on the rat skull which, in turn, were related to the point of inoculation. For vertical positioning, the top of the skull in the radiographs was used as a landmark.

Fifty-two tumor-inoculated rats (35 irradiated rats and 17 unirradiated controls) were used in this study. The irradiations were carried out on day 15 postinoculation. Animals were closely monitored after irradiation and were killed if they appeared to be neurologically disabled or moribund.

Dosimetric Measurements and Dose Distribution Simulations

Absolute dosimetric measurement utilized thermoluminescent dosimeters, whereas ion-chamber measurements were used to verify the dose rate during the experiment (relative measurements). The energy spectrum of the beam was calculated analytically using the code "Source" based on the code "Photon" (Chapman et al., 1988). The input parameters included the energy of the electron beam in the storage ring, ring current, wiggler design and its magnetic field, and beam filtration. The resulting median beam energies were 66 and 74 keV with the 0.25- and 0.51-mm copper filters, respectively.

The distribution of the dose from the microbeam arrays was evaluated at a spatial resolution of a few micrometers using the EGS4 Monte Carlo simulations code (Nelson et al., 1985). The code's recent upgrades were used in the simulations, including a subroutine to introduce the effect of linear polarization of the synchrotron X rays and the subroutine LSCAT for low-energy scattering (Namito et al., 1993, 1995). Simulations followed the basic system of Slatkin et al. (1992), which used an older version of the EGS4 code, as well as that of Orion et al. (2000). The simulations incorporated linear polarization of the synchrotron X rays (90% polarization) and the penumbra of the beam, caused by the 0.9 mm–wide horizontal beam spot located at 28 m from the collimator (which was, in turn, positioned about 9 cm for the center of the animal's head).

Histopathology

The brains of some of the MRT-treated rats, for which tissue collection became possible (9 of 35), were removed when the rats were killed, and the brains were fixed in 10% neutral buffered formalin. The fixed brain tissue was cut in the horizontal plane, embedded in paraffin, sectioned at 5- or 6-μm intervals, and stained with hematoxylin and eosin. Luxol fast blue stain was used to stain myelin. Tissue sections were coded. Histopathologic evaluation was carried out blind by 2 pathologists certified by the American Board of Pathologists.

MRI

The rationale for MRI was to verify complete ablation of the tumor and the integrity of the normal brain under MRT treatment. A Marconi Edge (Cleveland, Ohio) 1.5-tesla clinical scanner from the Magnetic Resonance Research Center of the State University of New York at Stony Brook was used. The system employed a coil custom-made for rat brain studies (Fiel and Button, 1990). This receive-only coil consisted of a 3-turn solenoid (4 cm in diameter) positioned orthogonal to the main field. Routine imaging included 1 mm–thick spin-echo acquisitions. The T1 sequence, used before and after the administration of gadolinium, employed TE (echo time) = 10 ms and TR (repetition time) = 500 ms. A double spin-echo sequence (TE = 20/80 ms, TR = 2000 ms) was used to obtain proton density and T2-weighted images (Gomori and Grossman, 1988).

Statistical Methods

Median survival time and 95% confidence intervals were estimated using the Kaplan-Meier method. These results were generated in S-Plus 2000 (Mathsoft, Inc., Cambridge, Mass.). Median survival times were calculated for each of the 7 beam spacings/dose configurations and for the defined categories (see "Results"). Because the data for the broad beams were only available up to 100 days postinoculation (Joel et al., 1990), their comparisons with other categories were made by censoring all groups at 100 days. Because no rats in the MRT groups were censored before 100 days postinoculation, it was possible to calculate the proportion surviving at 100 days and 95% confidence intervals by treating them as simple pro-

portions in StatXact-4 (Version 4.0.1, Cytel Software Corporation, Cambridge, Mass.). Time-to-event analyses were performed using log-rank tests. Comparisons of each configuration (7) with the control were conducted with separate log-rank tests, and the resulting P values were Bonferroni corrected; that is, they were compared with the Bonferroni-corrected *P* value cutoff for significance of 0.007 (0.05/7). Comparisons among all 7 configurations were also Bonferroni corrected with 7-choose-2 comparisons. The corrected cutoff for the significance was chosen to be $P = 0.0024$ (0.05/21). Comparisons among the categories (tolerable dose, high dose, all-MRT) and with the broad-beam results of Joel et al. (1990) and controls (Table 4), also performed using log-rank tests, were not Bonferroni corrected, mostly because some data were partially overlapping (the tolerable-dose with all-MRT data). The uncorrected *P* values are included in the Tables. Finally, for additional comparison with the broad beam data which ended at 100 days, we analyzed the survival curves of the categories, using log-rank tests, with all data censored at 100 days.

Results

Microbeam Dose Distributions from Monte Carlo Simulations

Microbeam dose distributions for the irradiations used in this work (27 μm and the beam spacings of 50, 75, and 100 μm) were calculated with the EGS4 Monte Carlo simulation code. The rat brain was simulated as a water cylinder 20 mm in diameter and 50 mm in length, covered with a 0.6 mm–thick skull. It was positioned horizontally in front of the array of vertical microbeams, 9 mm in width and 10.4 mm in height, which impinged on the side of the cylinder. The position of the center of the array was vertically at the midline of the cylinder and horizontally 9.5 mm shifted to one side (toward the rat's nose). Only every fifth beam in the array was simulated; the entire array was then produced by repeating, offsetting, and adding the beams. The data were taken for presentation depthwise in the center of the brain and laterally in the center of the array and the 2 edges. The volume from which the data were averaged was ±1 mm in depth, ±1 mm in height, and 15 microbeams in the lateral direction (1.5 mm for the 100-μm beams). The results are shown in Fig. 1. The distributions are displayed for 2 microbeams in the array and are normalized to the peak dose. The values of the valley doses, expressed as a percentage of the peak dose in the center and edge of the array and the average, are given in Table 1, together with the integrated dose of the microbeam array (as a percentage of the peak dose) and the full width of the valley at half depth. The significance of the valley dose is that it determines the survival of cells (for example, endothelial cells) between the microbeams, whereas the valley width may, in part, determine how many of these cells survive between 2 microbeams. The integrated dose of the microbeam array, calculated by averaging the dose distribution of the microbeam over 1 complete cycle (a width of the

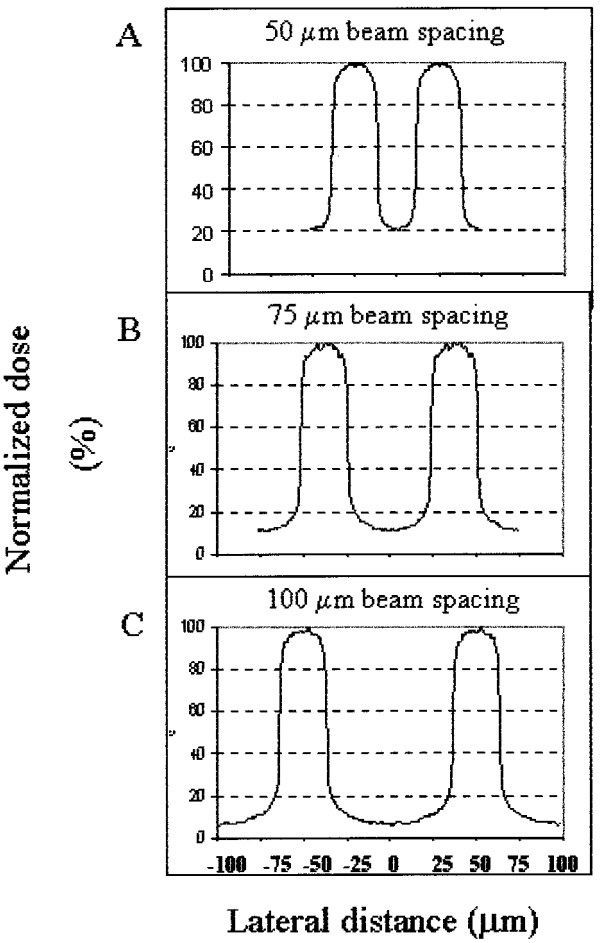

Fig. 1. Monte Carlo simulations of the dose distribution of microbeams in the different configurations of the rat i.c. 9LGS experiment. The 3 plots relate to microbeam arrays of the 27-μm beam width and the following beam spacings (center-to-center): 50 μm (A), 75 μm (B), and 100 μm (C).

Table 1. Monte Carlo simulation results for dose distribution of microbeam arrays (beam width of 27 μm) at the lateral center of the array and at the depth of the center of the brain

Beam spacing center to center (μm)	Valley dose as % of the peak in the center of array	Valley dose as % of the peak at the edge of array	Valley dose as % of the peak, averaged over the lateral profile of array	Integrated dose as % of the peak dose	Width of the valley in the center of array, full width at half depth (μm)
50	20.2	17.4	18.8	63	23
75	10.1	8.3	9.2	44	48
100	5.9	4.6	5.3	33	73

Table 2. Irradiation parameters and qualitative estimate of the degree of epilation for the individual configurations of MRT, together with dose distribution results from Monte Carlo simulations

Configuration, no. of rats, and category	Beam spacing center to center (μm)	In-slice skin-entrance dose (Gy)	In-slice dose at center of brain (Gy)	Valley dose at center of brain, averaged laterally (Gy)	Integrated dose at center of brain, averaged laterally (Gy)	Qualitative estimate of degree of epilation[a]
A (*n* = 5) High dose	50	150	108	20	68	++
B (*n* = 5) High dose	50	250	179	34	113	+++
C (*n* = 5) High dose	50	300	215	40	135	+++
D (*n* = 5) Tolerable dose	75	250	179	17	79	+
E (*n* = 6) High dose	75	300	215	20	95	++
F (*n* = 6) High dose	75	500	359	33	158	+++
G (*n* = 3) Tolerable dose	100	500	359	19	118	+
Unirradiated controls (*n* = 17)	N/A	N/A	0	0	0	0
Broad beams Joel et al., 1990 (*n* = 16)	N/A	N/A	22.5	N/A	22.5	Not known

Abbreviations: NA, not applicable

[a] +++, strong and permanent; ++, medium; +, small.

array equal to 1 beam spacing) reflects the average tissue dose and is significant for comparison with doses from broad beams.

Animal Survival as a Function of MRT Dose and Beam-Spacing Configurations

Rats were inoculated intracerebrally with 9LGS cells on day 0 and were irradiated with different MRT configurations (different beam spacings and doses) on day 15, when the tumors were approximately 4 mm in diameter. Thirty-five rats were irradiated in 7 configurations of A-F, which included beam spacings of 50, 75, and 100 μm, and in-slice entrance doses ranging from 150 to 500 Gy, as listed in Table 2. The irradiations were carried out in 4 different experimental periods within 11 months at the NSLS. In each experiment, the inoculated rats were randomized. The unequal number of rats in the configurations were caused by differences in the availability of animals in different experiments and by experimental difficulties such as machine breakdown or aberrant irradiations. The rats were observed for up to 500 days. Seventeen inoculated rats were used as unirradiated controls. Kaplan-Meier survival curves for these configurations, together with the curve of the unirradiated controls are shown in Fig. 2. Table 2 also presents the basic dosimetry results, together with a qualitative estimate of degree of epilation. Table 3 presents the proportion of rats surviving at 100 days and median survival values (postinoculation), together with their 95% confidence intervals. The latter ranged from 19 days in the unirradiated control group to 171 days in configuration D (75-μm beam spacing, 250-Gy dose). Individual comparisons for the 7 configurations and the controls, performed with the log-rank test, showed that all individual configurations were significantly different from the controls (*P* values of <0.007, the Bonferroni-corrected cutoff significance). However, in pairwise comparisons among the irradiated configurations, accounting for 21 comparisons, only 2 comparisons approached statistically significant differences using the Bonferroni-corrected *P* value cutoff of 0.0024, namely configuration B versus configuration D (*P* = 0.0027) and configuration C versus configuration D (*P* = 0.0027). This suggests that the 75-μm beam spacing and the 250-Gy dose produced longer survival than the 50-μm beam spacings at either the 250- or the 300-Gy dose. These results point to the larger toxicity on the brain from smaller beam spacings and/or higher doses (confirmed from histology, described below).

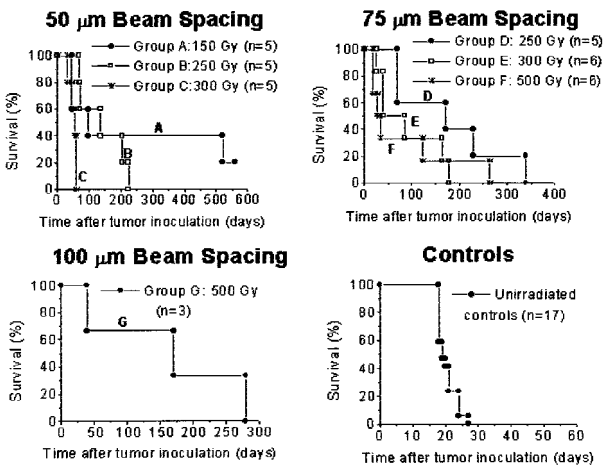

Fig. 2. Survival plots of the individual MRT configurations, together with a plot of the unirradiated controls.

In-Slice-, Valley-, and Integrated-Microbeam Doses in the Center of the Brain and the Tumor

The in-slice microbeams in tissue depths were calculated by subjecting the synchrotron X-ray spectrum to attenuation in 0.6-mm skull and 13-mm soft tissue for the center of the brain (Table 2). The calculations showed half-value layers of 13 mm for the skull and 30 mm for the soft tis-

Table 3. Median survival and proportion of rats surviving at 100 days for the different microbeam configurations of MRT, unirradiated controls, and broad beams of Joel et al. (1990)

Configuration, no. of rats, and category	Proportion of rats surviving 100 days postinoculation	95% CI for survival	Median survival (days)	95% CI for median survival
A (n = 5) High dose	0.40	(0.15, 0.95)	98	(45, NA)
B (n = 5) High dose	0.60	(0.05, 0.85)	136	(73, NA)
C (n = 5) High dose	0.00	(0.00, 0.52)	55	(46, NA)
D (n = 5) Tolerable dose	0.60	(0.15, 0.85)	171	(70, NA)
E (n = 6) High dose	0.33	(0.04, 0.78)	62.5	(40, NA)
F (n = 6) High dose	0.33	(0.04, 0.78)	31	(19, NA)
G (n = 3) Tolerable dose	0.67	(0.09, 0.99)	170	(39, NA)
Nonirradiated controls (n = 17)	0.00	(0.00, 0.16)	19	(18, 21)
Broad beams (n = 16) (Joel et al., 1990)	0.25	(0.07, 0.52)	33.5	(30, NA)

Abbreviations: CI, confidence interval; NA, not available (the upper limit was larger than the range of the data).

sue. The in-slice dose in the center of the tumor can be calculated by multiplying the doses by a factor of 0.91 for attenuation in an additional 4-mm depth of soft tissue. The valley doses at the center of the brain, also appearing in Table 2, were calculated using the incident in-beam doses, the percentage of valley doses from Table 1 (averaged over the lateral profile of the array), and attenuation of 0.6-mm skull and 13-mm soft tissue. Finally, Table 2 also includes the integrated MRT doses (in Grays) at the center of the brain.

Animal Survival for the 2 MRT Categories

The survival dependence on the 2 parameters of dose and beam spacings appear not to be strong enough to be detected within the statistics of the given number of animals in each configuration. However, if the effects are sought as a function of a single parameter (a "canonical" parameter) of MRT, the number of rats in the experiment could be large enough to measure the efficacy of MRT on that parameter. One such parameter is the valley dose of the dose distribution from the microbeam array. This parameter, which depends both on the beam spacing (Fig. 1) and the incident dose, clearly has a crucial role in determining the radiation effects of the microbeams as it determines the survival of the cells (for example, endothelial cells) between the microbeams. For this purpose, we chose a threshold of 19 Gy for the valley doses of the configurations (Table 2) to divide rats in 2 categories of tolerable dose and high dose (see rationale below). Configurations with a 19-Gy valley dose or lower (D and G) constituted the tolerable-dose category, whereas those with higher than a 19-Gy valley dose (A, B, C, E, and F) made up the high-dose category. This process of data averaging and reducing the number of variables to a single one (the valley dose) allowed us to maximize the power to detect meaningful differences among groups. The rationale for choosing the 19-Gy threshold for dividing the 2 categories was, first, the work of Joel et al. (1990), showing that a 22.5-Gy dose from a broad beam was only marginally tolerated by the rat brain. In that experiment, which is intensively compared with our experiment, the 22.5-Gy dose (at the center of the tumor)

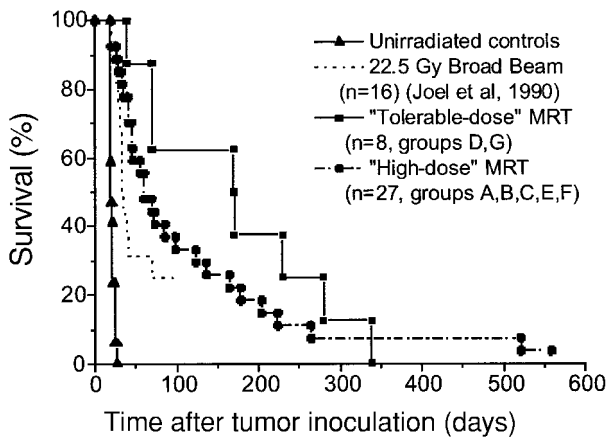

Fig. 3. Survival curves of rats receiving tolerable and high-dose MRT, the unirradiated controls, and the broad beams from Joel et al. (1990).

from a 250-kVp X-ray machine was given from the top, with the animal positioned prone and with a circular beam of 14 mm in diameter being used (Joel et al., 1990). Second, Calvo et al. (1988) reported that the doses of 250-kVp X rays that were given to the rat brain in a single exposure and produced 50% incidence of white matter necrosis in 39 and 52 weeks were 23.45 ± 0.49 Gy and 20.89 ± 0.91 Gy, respectively.

The assignment of the configurations to the 2 categories appears in Table 2. The number of the rats in the tolerable- and high-dose categories are 8 and 27, respectively. Fig. 3 presents the survival curves of the tolerable-dose and high-dose categories, the unirradiated controls from this work, and the broad-beam survival results of Joel et al. (1990). The median survival values and the percentage survival at 100 days postinoculation from these 4 groups and from all MRT results combined, together with their 95% confidence intervals, are presented in Table 4. Point estimates of median survival and proportion survival at 100 days for the rats treated with the tolerable dose and broad beams indicate that not only is the median survival 5-fold longer (170 days versus 33.5 days), but

Table 4. Median survival and proportion surviving at 100 days for the tolerable-dose and high-dose categories of microbeams and for broad beams

Group	No. of rats in group	Median survival in days postinoculation (95% CI)	Proportion surviving at day 100 postinoculation (95% CI)
Tolerable-dose MRT (optimal)	8	170 (70, NA)	0.63 (0.24, 0.91)
High-dose MRT (nonoptimal)	27	60 (45, 136)	0.33 (0.17, 0.54)
All MRT	35	70 (55, 170)	0.40 (0.24, 0.58)
Nonirradiated controls	17	19 (18, 21)	0.00 (0.00, 0.20)
Broad-beam treatment (Joel et al., 1990)	16	33.5 (30, NA)	0.25 (0.07, 0.52)

Abbreviations: See Table 3.

survival at 100 days is 2.5-fold larger (63% versus 25%). However, large confidence intervals qualify any claims of significance.

Comparisons of the survival curves from the categories listed in Table 4 were performed using the log-rank test for both the full data and data censored at 100 days. The results are presented in Table 5. They suggest that, first, the comparison of the survival curve for the complete data and data censored at 100 days for the tolerable-dose MRT versus the broad-beam irradiation were approaching significance ($P = 0.03$). However, the tolerable-dose versus high-dose survival curves potentially show only marginal, if any, significant differences for the full data ($P = 0.27$) and for the censored data, ($P = 0.14$). The smaller P value for the 100-day survival reflects the larger lead of the tolerable-dose survival at the earlier interval (<300 days), which is lost when the 2 curves cross at about 340 days (Fig. 3). Second, the superiority of the all-MRT category versus broad-beam treatment also approaches significance ($P = 0.06$). Third, rats in the tolerable-dose, high-dose, and all-MRT groups had significantly longer survival than did the control group, both for the full data ($P < 0.001$) and for data censored at 100 days ($P < 0.001$). Fourth, the high-dose category appeared not to significantly differ from the broad-beam group for both full data and censored data ($P = 0.19$).

We note that the 63% survival of the tolerable-dose category at 100 days postinoculation is comparable to 60% from the boron neutron capture therapy experiment reported by Joel et al. (1990).

Histopathology of Brain Tissue

Histologic studies for the MRT-treated animals were carried out on only 9 available samples. The most important finding was that in 8 samples, where the tumors were ablated with MRT, no tumor residues were visualized. However, some of the histologic features observed may be related to the ablated tumors, namely microcalcifications and, infrequently, increased vascularization. Second, the brain tissues in all MRT-treated rats, including those in the high-dose category, showed remarkably low levels of damage. None of the brains showed either gray matter necrosis, depletion of nerve cells, vacuolar changes, or demyelinization. In the high-dose category, the predominant damage was white matter necrosis, which was observed in 4 of 7 samples examined (Table 6). Other histologic abnormalities, also limited to the high-dose category, were small perivascular hemorrhages, intimal thickening with or without microcalcification, and necrosis of the vascular wall. In the tolerable-dose category, however, the only lesions observed were foci of hypervascularization, microcalcification, and minor edema. These lesions may mark the sites of ablated tumors.

The tumor in the only tumor-containing sample (#6B in Table 6, irradiated with 50-μm beam spacing/300 Gy, harvested at day 48 postinoculation) was well circumscribed with infiltrating borders. It was composed of spindle cells with a storiform pattern of growth, a high nuclear-to-cytoplasmic ratio, vacuolated/reticular chromatin, frequent small nucleoli, and high mitotic activity. Occasional large pleomorphic cells were observed, some of which were multinucleated. Regional tumor necrosis was evident. There was peritumoral necrosis and an increase in the vascularity in the peritumoral zone. The capillaries adjacent to the tumor were surrounded by a cuff of tumor cells. All these features are those of a high-grade glioma.

Figs. 4-7 show photomicrographs of certain segments of 4 different brain samples, all depicted at ×100 magnification. Fig. 4 shows the tumor-bearing sample 6B of configuration C (high-dose, 50-μm beam spacing, 300-Gy dose) illustrating the margin between the normal brain and the tumor. Fig. 5 shows sample 15A of configuration F (also high-dose, 75-μm beam spacing, 500-Gy dose), exhibiting white matter necrosis, which may be considered more significant than the other types of brain damage observed in the MRT-irradiated rat brain samples evaluated. Fig. 6 shows sample 5F of configuration D (tolerable dose, 75-μm beam spacing, 250-Gy dose). The illustration shows very little, if any, damage, as it can be judged by comparing it with the histology slide from a normal, unirradiated rat brain shown in Fig. 7. We note that the samples were taken at 398 days postinoculation from rats aged about 480 days for the MRT-treated brain #5F (Fig. 6) and aged 1 year for the normal, untreated brain (Fig. 7).

MRI of Untreated and MRT-Treated Rat Brains

As indicated above, MRI was carried out as an additional method of examining MRT-treated rat brains for complete tumor ablation and lack of brain damage. Two rats with 9LGS were imaged. An untreated rat (Rat 1) was imaged at day 14 after inoculation, and an MRT-treated rat (Rat 2) was imaged 4 months postinoculation (Fig. 8). T2-weighted images were obtained before administration of

Table 5. Log-rank tests of the difference in survival curves between MRT categories, unirradiated controls, and broad beams of Joel et al. (1990) for the complete data set and for data censored at 100 days

Group 1	Group 2	*P* value for complete data[a]	*P* value for data censored at 100 days[a]
Tolerable-dose MRT (*n* = 8)	Unirradiated controls, MRT (*n* = 17)	<0.001	<0.001
	Broad beams (*n* = 16)	0.03	0.03
	High-dose MRT (*n* = 27)	0.27	0.14
High-dose MRT (*n* = 27)	Unirradiated controls, MRT	<0.001	<0.001
	Broad beams	0.19	0.19
All MRT (*n* = 35)	Unirradiated controls, MRT	<0.001	<0.001
	Broad beams	0.06	0.06

[a]Reported *P* values are uncorrected for multiplicity.

Table 6. Results of histologic studies of the MRT-treated rat brain

Configuration/ dose/beam spacing/ category	Sample no.	Days postinoculation	Residual tumor/ tumor necrosis	White matter necrosis[a]	Micro-calcification[a]	Vascularization[a]	Local minor edema[a]
C/300 Gy/ 50 μm/High dose	6B	48	Gross tumor/small areas of necrosis	+	+	++ Peritumor	++
	10B	48	None	+	+	+++ With calcification	+
B/250 Gy/ 50 μm/High dose	11G	68	None	+	+++	+	None
	13G	200	None	None	+++	None	None
	19G	134	None	None	+	+	+
	21G	72	None	None	+++	+++	++
F/500 Gy/ 75 μm/High dose	15A	120	None	++	++	+++	+
D/250 Gy/75 μm/ Tolerable dose	5F	398	None	None	+++	None	+
G/500 Gy/100 μm/ Tolerable dose	10E	144	None	None	+++	None	None

Only 1 of the 9 brains studied included tumor. None of the samples showed depletion of nerve cells, demyelinization, or vacuolarization.

[a]+++, strong; ++, medium; + small.

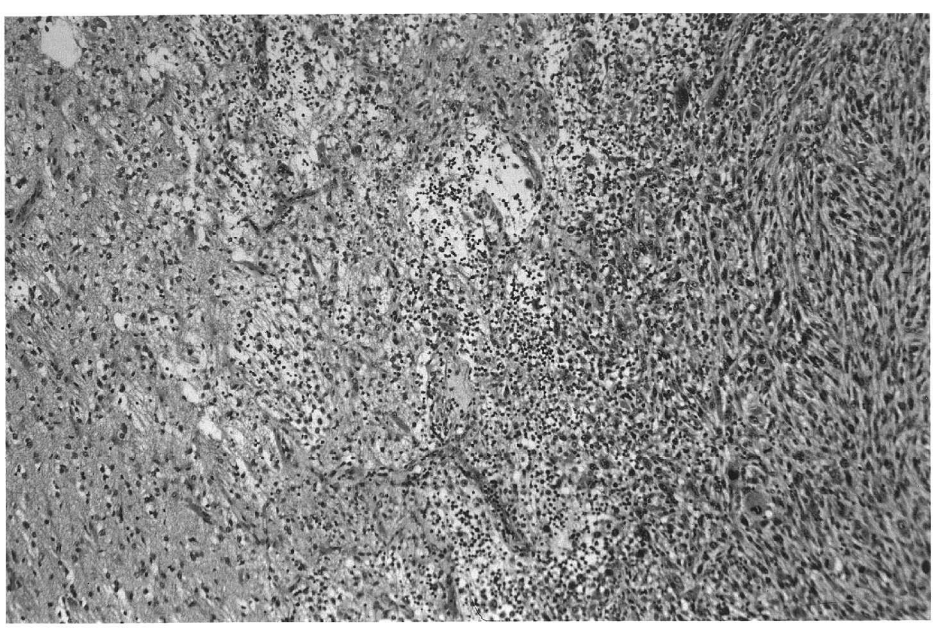

Fig. 4. Photomicrograph of a zone of rat cerebrum (sample 6B of Table 6), treated with configuration C, in which the rat brain was irradiated with 27 μm–wide microbeams of 50-μm center-to-center spacing at an in-slice entrance dose of 300 Gy (the high-dose category). The figure shows the edge of the tumor. Original magnification ×100.

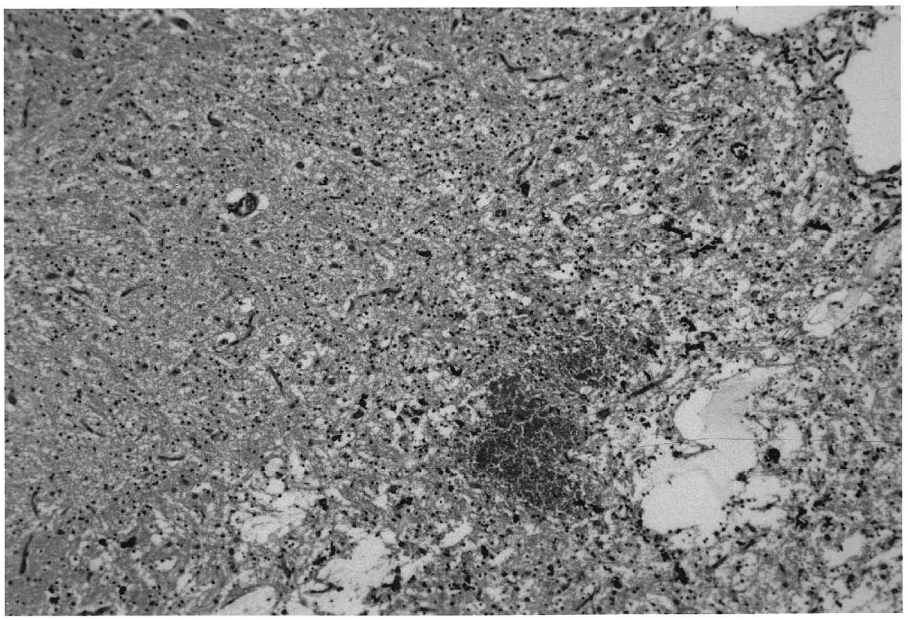

Fig. 5. Photomicrograph of a zone of rat cerebrum (sample 15A) treated with configuration F. MRT was with 75-μm beam spacing and at a 500-Gy dose (high-dose category). The figure shows regions of white matter necrosis. Original magnification ×100.

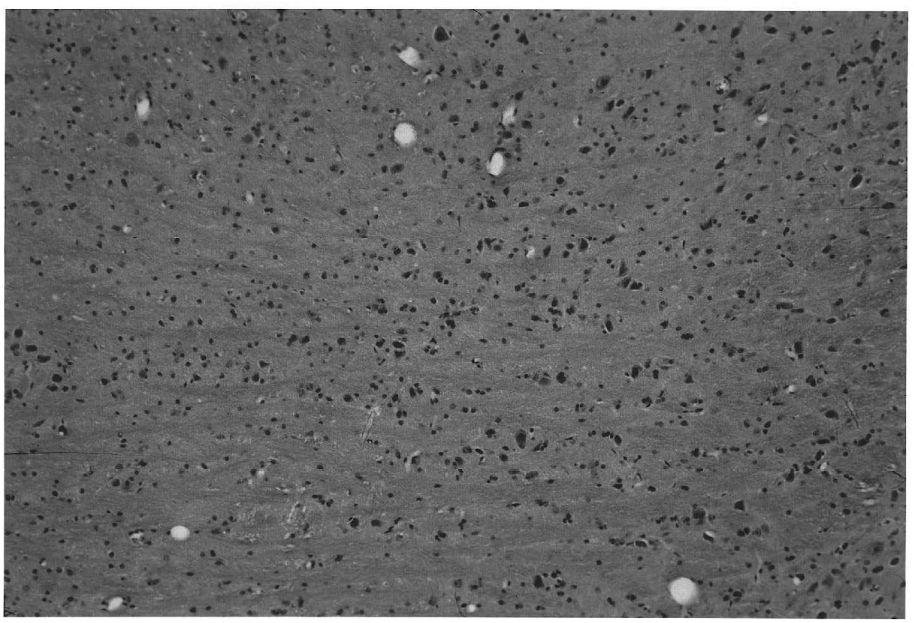

Fig. 6. Photomicrograph of a zone of rat cerebrum (sample 5F) treated with configuration D. MRT was with a 75-μm beam spacing at a 250-Gy dose (tolerable-dose category). No damage was observed. The sample was taken at 398 days postinoculation; the rat was approximately 480 days old. Original magnification ×100.

gadolinium, and T1-weighted images were obtained afterwards. All images were at 1-mm axial sections. The tumor in Rat 1 is represented by an area of enhanced contrast in the left hemisphere. Scars were evident in the tumor zone of the brains of the microbeam-treated rat (Fig. 8). The midline of the brain was not displaced laterally in these animals. In the T2-weighted images, the tumor zone was visualized as a scar that appeared isointense relative to the surrounding normal brain (a ventricle). There was no evidence of white matter necrosis or edema in the treated rat, which would have been marked by gadolinium leakage. The studies indicate that, at least under some conditions, MRT may leave little normal brain damage and few traces of tumor detectable by MRI.

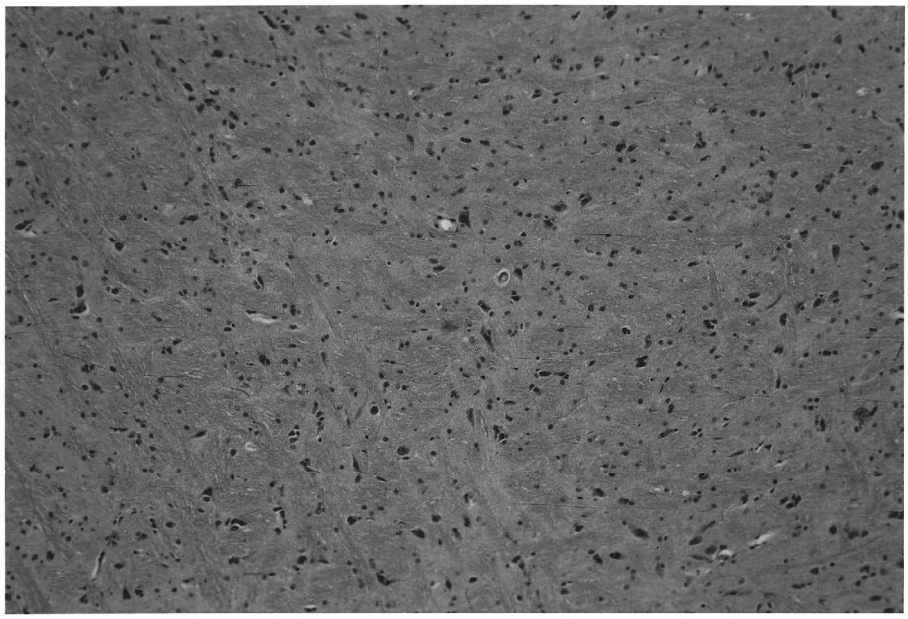

Fig. 7. Photomicrograph of a zone of a normal, unirradiated rat cerebrum shown for comparison with Fig. 6 to demonstrate that there is little if any difference. The sample was taken from a 1-year-old rat. Original magnification ×100.

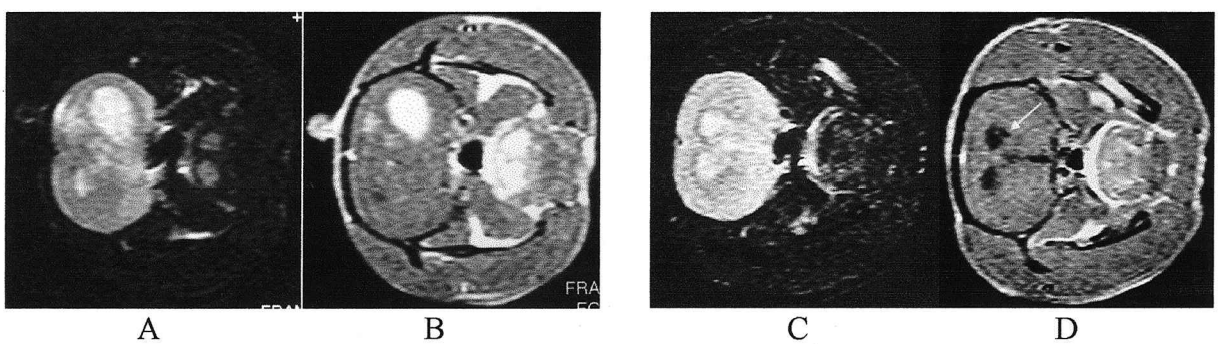

Fig. 8. MRI of 9LGS-inoculated rats. A. T2-weighted image of the untreated rat, Rat 1, before the administration of the gadolinium (Gd) contrast agent. B. T1-weighted image of Rat 1 after the administration of the Gd agent. C. T2-weighted image of the MRT-treated rat, Rat 2, before Gd. D. T1-weighted image of Rat 2 after Gd administration. In the untreated rat, the tumor and surrounding area (edema) appear bright on the T2 image (A), whereas the post-Gd T1 image shows the boundary of the tumor (B). In the MRT-treated rat, the hemispheres appear to be symmetrical on the T2 image (C), whereas the post-Gd T1 image (D) reveals no residual tumor or necrosis. A tumor scar is evident in the treated rat (arrow). It is not a normal brain scar because such a scar would have taken up Gd.

Discussion

Our findings suggest that unidirectional MRT, administered in a single exposure over a certain range of doses and beam spacings, can control a sizable proportion of i.c. rat 9LGS (judging from up to ~200 days postirradiation) without producing major damage to the brain. Furthermore, MRT still spares the normal brain when the beam spacing is only about twice that of the beam width (see configuration A in which the 27-μm beam width, 50-μm beam spacing, and 150-Gy dose allowed 40% of the rats to survive to 500 days postinoculation). Another important finding is that the sparing effect of MRT seems to depend mostly on the valley dose and little on the peak dose (within certain limits). The brain-sparing effect vanishes (measured by the onset of the appearance of white matter necrosis) only when the valley dose approaches the tissue tolerance to broad beams (see Table 2). The process in which the tumors disappear also seems to be different with MRT compared with broad-beam treatment. In MRT, the tumor seems to be resorbed gradually, leaving very little detectable residues. We note that, in most of our configurations, the doses were too large and/or the beam spacings were too small.

The following compares the histologic findings in rats from the tolerable-dose MRT with those from an earlier study by colleagues in our department utilizing conventional broad-beam X rays (Joel et al., 1990). Their histologic analysis, reported by Coderre et al. (1994b), was limited to 2 rats 1 year after irradiation. The emphasis in

the study was on examining the integrity of the blood-brain barrier by determining the extent of leakage of horseradish peroxide. First, in contrast to the MRT-treated brains in our study in which the tumor does not leave much residue, the broad-beam effect on the tumor in their study is very different: "The tumor scar is large and the dorsal portions of the cortex and the corpus callosum are severely compromised. The striatum is virtually destroyed and there is significant hydrocephalus as demonstrated by the greatly enlarged ventricle" (Coderre et al., 1994b). Second, in contrast to MRT-treated brains where there is no gray matter necrosis nor depletion of nerve cells, even in the high-dose categories, they observed: "The cortex and striatum in the irradiated region were depleted in neurons and the scar replacing the tumor was cystic in nature. The corpus callosum was severely atrophied." Other brain damage they reported included "…generalized neuronal atrophy, gliosis, demyelinization, severe hydrocephalus ex vacuo." Finally, in contrast to MRT in which vascular damage was minor and was limited to the high-dose category, they observed that "…there was disruption of the fine capillary network with vascular leakage."

In the tolerable-dose category, there were several late deaths (deaths beyond 150 days) that could not be explained by the assessed histologic brain damage. Similar deaths in the studies of i.c. 9LGS tumors were observed by boron neutron capture therapy and broad X-ray beams (Joel et al., 1990) and by MRT (Laissue et al., 1998). One possible explanation of this effect is that the irradiated volume of the rat brain in all these irradiations was large, constituting a significant size of the entire brain. For our microbeam irradiations, the proportion of the rat brain irradiated, considering the entire depth of the brain in the path of the array as irradiated, was about 50% (9-mm lateral width of the brain, times its entire depth, times almost its entire height). This is a very large irradiation volume compared with clinical radiotherapy where the irradiated volume around a typical brain tumor of 4 cm in diameter constitutes a much smaller portion of the brain. Other possible explanations could be that the brain damage was not demonstrable histologically. We note that our survivals reached 560 days postinoculation, which means the rats were about 650 days of age. This age approaches the median lifespan of Fischer 344 rats, which is reported by Armbrecht et al. (1988) to be 24 months. Therefore, a third possible explanation for these late deaths could be unrelated morbidities.

A qualitative estimate can be made for the therapeutic index of the MRT in the tolerable-dose category versus that in the 22.5-Gy broad-beam treatment (Coderre et al., 1994b; Joel et al., 1990). If these 2 treatments were comparable regarding their damage to the normal brain, we could calculate their relative therapeutic index by comparing the ratio of their therapeutic efficacies. However, because the toxicity to the brain from broad beams is much greater than that from tolerable-dose MRT, such a comparison would favor broad-beam treatment. Nevertheless, using the median survival time as an indicator of therapeutic efficacy, the tolerable dose of MRT has an advantage of 170 days versus 33.5 days over the broad-beam therapy, a 5-fold advantage. When the percent survival at 100 days is used as an indicator, the advantage of the tolerable dose MRT would be 2.5-fold (63% versus 25%).

To evaluate the rat-brain tolerance-dose ratio between microbeams and the broad beams, we assumed a 22.5-Gy broad-beam tolerance dose. For microbeams, we assumed that the tolerance dose was the same as the integrated dose (defined above) for the tolerable-dose category. The latter was calculated as a weighted average of the integrated doses of the 2 configurations constituting the tolerable-dose category (D and G), with the weighting factors being the number of rats in each configuration. The result was a 94-Gy integrated dose in the center of the brain for the tolerable-dose category which, when compared with 22.5 Gy for the broad beams, represented a net 4.2-fold tolerance advantage for microbeams. This suggests that the tissue-sparing effect of MRT is not merely due to a "volume factor" (defined below) because that factor was taken into account when using the integrated dose instead of the in-slice doses of MRT. In other words, the sparing effect of microbeams in normal tissues cannot be attributed only to a smaller integrated dose of the microbeams compared with the broad beams for the same incident doses; there must be a real biological sparing effect. The volume factor is defined as the ratio of in-slice dose to integrated dose. It could relate to an effect of small, but still macroscopic beams. That effect is that the threshold dose for causing normal tissue damage increases as the volume of the tissue irradiated decreases, within macroscopic limits (Withers et al., 1988). That phenomenon, which is the basis for "grid radiotherapy" (Mohiuddin et al., 1996), spares the normal tissue when the beam is segmented into regions of centimeters to millimeters in size. Therefore, the tissue-sparing effect of microbeams appears to combine a volume factor with a biologic microbeam effect, whereas the grid effect could result entirely from a volume factor.

The biologic portion of the tumoricidal effect of unidirectional microbeams may include the inhibition by MRT of the vascular regeneration within the tumor. It is thought that differences between the vasculature of normal and neoplastic tissues make tumors more susceptible to some therapeutic modalities (Denekamp 1992). These differences may include abnormal properties of tumor vasculature in more rapid endothelial cell proliferation (Denekamp, 1984) and a poorly developed vessel structure (Denekamp, 1984; Horbelt et al., 1999). It is thought that the vasculature plays an important role in mediating the radiation-induced damage in the CNS (Morris et al., 1996; van der Kogel et al., 1996). Treatment of the rat spinal cord with boron neutron capture therapy, using a boron compound that stayed in the blood vessels, produced pathology similar to that observed after conventional irradiation with 250-kVp X rays where both the vasculature and the CNS parenchyma were uniformly irradiated (Morris et al., 1996). Both the timing and patterns of necrosis were similar, suggesting that the radiation damage to the vasculature alone is sufficient to produce the same CNS damage caused by irradiating the parenchyma.

Experimental evidence that the tumoricidal effect of unidirectional MRT cannot be attributed to direct tumor cell lethality may come from a small pilot clonogenic

study by D. N. Slatkin, J. A. Coderre, D. D. Joel, M. S. Makar, P. Spanne, F.A.D. (unpublished data, 1992). Five rats with intracerebral 9LGS were irradiated with bidirectional MRT at doses that previously had ablated about 50% of the tumors. The rats were killed 5 min after irradiation, the tumors were excised and trypsinized, and the cells were plated in a clonogenic assay. About 2% of the clonogenic cells survived. This is a large survival, compared with about 0.2% (Leith et al., 1975) from broad-beam treatment at a therapeutic dose approaching 50%. It suggests that the tumoricidal effect of MRT cannot be explained exclusively by the death of tumor cells, and other mechanisms must be involved. One such mechanism could be the failure of the tumor microvasculature to recover from microbeam irradiation (in contrast to the microvasculature of the normal tissue that perhaps does recover), leading to the loss of tumor blood perfusion and, ultimately, to tumor death.

In conclusion, our findings suggest that single-fraction, unidirectional MRT may be superior to single-fraction conventional radiotherapy in treating i.c. rat 9LGS experimental tumors. We expect to be able to exploit further the superiority of MRT over broad-beam radiotherapy by optimizing the beam width and spacing of the microbeams, using dose fractionation, and using bidirectional and tridirectional MRT.

Acknowledgments

We thank J.A. Coderre for advice on the experimental design; D.D. Greenberg, M.S. Makar, G. Mpozios, and L. Rigon for help with dosimetry; I. Orion, X.-Y. Wu, and Z. Zhong for help during the irradiations; N. Peress for advice on pathology; K.A. Bonti, W. Estrada, X. Huang, M. Kershaw, D. Lombardo, C. Rissland, P. Sathé, B. Scharf, and K. Trandem for help with animal studies; and V. Geronim and H. Li for help with MR imaging. We thank L. Chang, A.Z. Diaz, T. Ernst, S.J. Gatley, J.N. Gilbert, D.D. Joel, A.N. Sawchuk, R.B. Setlow, D.N. Slatkin, F. Telang, W.C. Thomlinson, A.D. Woodhead, and R. Yakupov for discussions and/or for help with the manuscript. We also thank L. Chang, P. Paul, and N.D. Volkow for support and encouragement, and Emtron Hybrids, Inc., Yaphank, N.Y., for a stipend (to J.T.).

References

Armbrecht, H.J., Strong, R., Boltz, M., Rocco, D., Wood, W.G., and Richardson, A. (1988) Modulation of age-related changes in serum 1,25-dihydroxyvitamin D and parathyroid hormone by dietary restriction of Fischer 344 rats. *J. Nutr.* **118**, 1360-1365.

Central Brain Tumor Registry of the US (CBTRUS) (2000, Chicago, Ill.) Statistical Report: Primary Brain Tumors in the United States, 1992-1997. Central Brain Tumor Registry of the United States.

Calvo, W., Hopewell, J.W., Reinhold, H.S., and Yeung, T.K. (1988) Time- and dose-related changes in the white matter of the rat brain after single doses of X rays. *Br. J. Radiol.* **61**, 1043-1052.

Chapman, L.D., Gmür, N.F., Lazarz, N., and Thomlinson, W. (1988) Photon: A program for synchrotron radiation dose calculations. *Nucl. Instrum. Methods Phys. Res.* A266, 191-194.

Coderre, J.A., Button, T.M., Micca, P.L., Fisher, C.D., Nawrocky, M.M., and Liu, H.B. (1994a) Neutron capture therapy of the 9L rat gliosarcoma using the p-boronophenylalanine-fructose complex. *Int. J. Radiat. Oncol. Biol. Phys.* **30**, 643-652.

Coderre, J., Rubin, P., Freedman, A., Hansen, J., Wooding, T.S., Joel, D., and Gash, D. (1994b) Selective ablation of rat brain tumors by boron neutron capture therapy. *Int. J. Radiat. Oncol. Biol. Phys.* **28**, 1067-1077.

Denekamp, J. (1984) Vascular endothelium as the vulnerable element in tumours. *Acta Radiol. Oncol.* **23**, 217-225.

Denekamp, J. (1992) Inadequate vasculature in solid tumours: Consequences for cancer research strategies. *BJR Suppl.* **24**, 111-117.

Dilmanian, F.A., Morris, G.M., Le Duc, G., Huang, X., Ren, B., Bacarian, T., Allen, J.C., Kelef-Ezra, J., Orion, I., Rosen, E.M., Sandhu, T., Sathé, P., Wu, X.Y., Zhong, Z., and Shivaprasad, H.L. (2001) Response of avian embryonic brain to spatially segmented X-ray microbeams. *Cell. Mol. Biol.* **47**, 485-494.

Fiel, R.J., and Button, T.M. (1990) Magnetic resonance imaging of small laboratory animals. *Lab. Anim. Sci.* **40**, 215-216.

Gomori, J.M., and Grossman, R.I. (1988) Mechanisms responsible for the MR appearance and evolution of intracranial hemorrhage. *Radiographics* **8**, 427-440.

Horbelt, D.V., Roberts, D.K., Parmley, T.H., Delmore, J.E., and Walker-Bupp, N.J. (1999) Ultrastructural interactions in the microvasculature of human endometrial adenocarcinoma. *Oncology* **73**, 76-86.

Joel, D.D., Fairchild, R.G., Laissue, J.A., Saraf, S.K., Kalef-Ezra, J.A., and Slatkin, D.N. (1990) Boron neutron capture therapy of intracerebral rat gliosarcomas. *Proc. Natl. Acad. Sci. U.S.A.* **87**, 9808-9812.

Laissue, J.A., Geiser, G., Spanne, P.O., Dilmanian, F.A., Gebbers, J.O., Geiser, M., Wu, X.Y., Makar, M.S., Micca, P.L., Nawrocky, M.M., Joel, D.D., and Slatkin, D.N. (1998) Neuropathology of ablation of rat gliosarcomas and contiguous brain tissues using a microplanar beam of synchrotron-wiggler-generated X rays. *Int. J. Cancer* **78**, 654-660.

Laissue, J.A., Lyubimova, N., Wagner, H.-P., Archer, D.W., Slatkin, D.N., di Michiel, M., Nemoz, C., Renier, M., Brauer, E., Spanne, P.O., Gebbers, J.-O., Dixon, K., and Blattmann, H. (1999) Microbeam radiation therapy. In: Barber, H.B., and Roehrig, H. (Eds.), Medical Applications of Penetrating Radiation. Proceedings of SPIE, Vol. 3770. pp. 38-45.

Laissue, J.A., Blattmann, H., Di Michiel, M., Slatkin, D.N., Lyubimova, N., Guzman, R., Zimmermann, W., Birrer, S., Bley, T., Kircher, P., Stettler, R., Fatzer, R., Jaggy, A., Smilowitz, H.M., Brauer, E., Bravin, A., Le Duc, G., Nemoz, C., Renier, M., Thomlinson, W., Stepanek, J., and Wagner, H.P. (2001) The weanling piglet cerebellum: A surrogate for tolerance to MRT (microbeam radiation therapy) in pediatric neuro-oncology. In: Medical Applications of Penetrating Radiation II. Proceedings of SPIE, Vol. 4508. In Press.

Leith, J.T., Schilling, W.A., and Wheeler, K.T. (1975) Cellular radiosensitivity of a rat brain tumor. *Cancer* **35**, 1545-1550.

Mohiuddin, M., Stevens, J.H., Reiff, J.E., Huq, M.S., and Suntharalingam, N. (1996) Spatially fractionated (GRID) radiation for palliative treatment of advanced cancer. *Radiat. Oncol. Invest.* **4**, 41-47.

Mornex, F., Nayel, H., and Taillandier, L. (1993) Radiation therapy for malignant astrocytomas in adults. *Radiother. Oncol.* **27**, 181-192.

Morris, G.M., Coderre, J.A., Bywaters, A., Whitehouse, E., and Hopewell, J.W. (1996) Boron neutron capture irradiation of the rat spinal cord: Histopathological evidence of a vascular mediated pathogenesis. *Radiat. Res.* **146**, 313-320.

Namito, Y., Ban, S., and Hirayama, H. (1993) Implementation of linearly-polarized photon scattering into the EGS code. *Nucl. Instrum. Methods Phys. Res.* **A332**, 277-283.

Namito, Y., Ban, S., Hirayama, H., Nariyama, N., Nakashima, H., Nakane, Y., Sakamoto, Y., Sasamoto, N., Asano, Y., and Tanaka, S. (1995) Compton

scattering of 20- to 40-keV photons. *Phys. Rev.* **A51**, 3036-3043.

Nelson, W.R., Hirayama, H., and Rogers, D.W.O. (1985) *The EGS4 Code System: SLAC 265*. Stanford, CA: Stanford Linear Accelerator Center.

Orion, I., Rosenfeld, A.B., Dilmanian, F.A., Telang, F., Ren, B., and Namito, Y. (2000) Monte Carlo simulation of dose distributions from a synchrotron-produced microplanar beam array using the EGS4 code system. *Phys. Med. Biol.* **45**, 2497-2508.

Schmidek, H.H., Nielson, S.L., Schiller, A.L., and Messer, J. (1971) Morphological studies of rat brain tumors induced by N-nitrosomethylurea. *J. Neurosurg.* **34**, 335-340.

Slatkin, D.N., Spanne, P., Dilmanian, F.A., and Sandborg, M. (1992) Microbeam radiation therapy. *Med. Phys.* **19**, 1395-1400.

Slatkin, D.N., Spanne, P.O., Dilmanian, F.A., Gebbers, J.-O., and Laissue, J.A. (1995a) Subacute neuropathological effects on rats of microplanar beams of x-rays from a synchrotron wiggler. *Proc. Natl. Acad. Sci. U.S.A.* **92**, 8783-8787.

Slatkin, D.N., Dilmanian, F.A., Nawrocky, M.M., Spanne, P., Gebbers, J.-O., Archer, D.W., and Laissue, J.A. (1995b) Design of a multislit, variable width collimator for microplanar beam radiotherapy. *Rev. Sci. Instrum.* **66**, 1459-1460.

van der Kogel, A.J., Kleiboer, B.J., Verhagen, I., Morris, G.M., Hopewell, J.W., and Coderre, J.A. (1995) White matter necrosis of the spinal cord: Studies on glial progenitor survival and selective vascular irradiation. In: Hagen, U., Jung, H., and Streffer, C. (Eds.), *Radiation Research 1895-1995*, Vol. 2. *Proceedings of the Tenth International Congress of Radiation Research*. Wurzburg, Germany: ICRR Society. pp. 769-772.

Winick, H. (1980) Properties of synchrotron radiation. In: Winick, H., and Doniach, S. (Eds.), *Synchrotron Radiation Research*. New York: Plenum Press. pp. 11-25.

Withers, H.R., Taylor, J.M.G., and Maciejewski, B. (1988) Treatment volume and tissue tolerance. *Int. J. Rad. Oncol. Biol. Phys.* **14**, 751-759.